Groundwater potential zonation in Sarpang District, Bhutan, using geographic information system, remote sensing, and the analytical hierarchy process

By

Rinchen Penjor

Thesis
Submitted to Flinders University
for the degree of

Master of Science (Water Resources Management)

College of Science and Engineering
May 30, 2025

CONTENTS

ABSTRACT ..... **III**
DECLARATION ..... **IV**
ACKNOWLEDGEMENTS ..... **V**
LIST OF FIGURES ..... **VI**
LIST OF TABLES ..... **VII**
1. INTRODUCTION **1**
2. STUDY AREA **5**
2.1. Location 5
2.2. Climate and hydrology 5
3. MATERIAL AND SOURCES **7**
4. METHODOLOGY **8**
4.1. Selection of groundwater-influencing factors 8
4.2. Application of Analytical Hierarchy Process 9
4.3. Weighted overlay analysis 16
5. RESULTS AND DISCUSSION **17**
5.1. Geology 17
5.2. Lineament density 18
5.3. Slope 19
5.4. Rainfall 20
5.5. Drainage density 21
5.6. Soil 22
5.7. Land use land cover 23
5.8. Groundwater potential map 24
5.9. Conformity with Electrical Resistivity Tomography test 26
6. UNCERTAINTY AND LIMITATIONS **29**
7. CONCLUSION AND RECOMMENDATIONS **32**
REFERENCES **33**
APPENDICES **39**

ABSTRACT

Globally, groundwater is gaining importance as surface water sources decline due to climate change and overexploitation. In Bhutan, despite the perceived abundance of surface water, seasonal shortages, drying sources, and limited infrastructure highlight the need for alternative resources such as groundwater. However, comprehensive groundwater assessments are limited. The purpose of this study is to overcome that gap by using a Multi-Criteria Decision Analysis approach, combining GIS, Remote Sensing and the Analytical Hierarchy Process to delineate groundwater potential zones in Sarpang District. The analysis indicates high recharge potential in southern Sarpang, which is consistent with Electrical Resistivity Tomography test results at two out of three test sites, supporting the effectiveness of the analytical hierarchy process (AHP) as a preliminary and cost-efficient tool. Still, the approach depends heavily on expert judgment and generalized datasets, which may limit the accuracy of the results. Field-based validation is therefore essential for ensuring the reliability of results and guiding sustainable groundwater development, especially in light of large-scale initiatives such as the Gelephu Mindfulness City, which is expected to drive significant population growth, urban expansion and increased water demand. Such developments require reliable groundwater assessments to ensure sustainable resource management and long-term water security.

DECLARATION

I certify that this thesis does not incorporate without acknowledgment any material previously submitted for a degree or diploma in any university; and that to the best of my knowledge and belief it does not contain any material previously published or written by another person except where due reference is made in the text.

Signed: RINCHEN PENJOR

Date: May 30, 2025.

ACKNOWLEDGEMENTS

I sincerely thank everyone who contributed to the successful completion of this research, *"Groundwater Potential Zonation in Sarpang District, Bhutan, Using GIS, Remote Sensing, and the Analytical Hierarchy Process,"* undertaken as a major component of my Master of Science in Water Resources Management.

To begin with, I am sincerely thankful to my supervisor, Professor Okke Batelaan, for his guidance, encouragement, and valuable feedback at every stage of the research. His expertise and support were instrumental in shaping this work. In addition to supervising my research, he also contributed as one of the experts in assigning weights to the groundwater-influencing factors for the Analytical Hierarchy Process (AHP) pairwise comparison, for which I am deeply grateful.

I extend my heartfelt thanks to the expert participants, Dr. Stephen Fildes and Mr. Langa Dorji, who generously contributed their time and knowledge by providing weights for the pairwise comparison of groundwater-influencing factors. I am especially grateful to Dr. Stephen for his additional guidance in helping me understand and apply the AHP with clarity and precision.

I am deeply grateful to my family for their steadfast support, enduring patience, and constant motivation throughout this journey. Their unwavering belief in me provided the strength and clarity I needed to stay focused.

This research has been one of the most enriching experiences of my academic journey, deepening both my technical understanding and appreciation of the complex challenges in groundwater management. I am truly grateful to everyone who played a part in this endeavour.

LIST OF FIGURES

Figure 1. A comprehensive map of the Sarpang district study area, generated using the SRTM Global Digital Elevation Model (DEM). 5

Figure 2: (a) Monthly average minimum and maximum temperatures, and (b) monthly and annual rainfall from 1996 to 2024, recorded at the Bhur Weather Station. Data source: National Centre for Hydrology and Meteorology (NCHM, 2024). 6

Figure 3: Overview of the methodology used for groundwater potential mapping. 8

Figure 4: Frequency of groundwater influencing factors used for 21 groundwater potential studies conducted in sub-Indian continent and African countries, using GIS, RS and AHP. 9

Figure 5: Map showing the geological features of the study area, adapted from Long et al. (2011). 18

Figure 6: Lineament and lineament density map derived from 30m resolution SRTM 1 Arc-Second Global DEM. 19

Figure 7: Slope map based on 30 m resolution SRTM 1 Arc-Second Global DEM. 20

Figure 8: Sarpang district rainfall map derived from WorldClim version 2.1 climate with dataset from 1970-2000. 21

Figure 9: Drainage network and drainage density map of Sarpang district derived from SRTM 1 Arc-Second Global DEM. 22

Figure 10: Soil types of the study area, Sarpang district (NSSC, 2024). 23

Figure 11: Land use land cover types of Sarpang district derived from LULC map of NLCS, 2016. 24

Figure 12: Groundwater potential map of Sarpang district categorized into three zones based on 55.8% consensus weights scoring from four expert participants. 25

Figure 13: 3-D inversion results showing subsurface layers at (a) Pelrithang, (b) Dzomlingthang, and (c) Lekithang. Source: DGM (2022) 27

Figure 14: Comparison of Electrical Resistivity Tomography (ERT) test locations with AHP-derived groundwater potential zones. 28

Figure 15: Groundwater potential zones generated using individual AHP scores (normalized eigenvalues in Table 3) from four experts (E-1, E-2, E-3, and E-4). 30

LIST OF TABLES

Table 1. A numerical scale used for pairwise comparisons in AHP (Saaty, 1977) 10

Table 2. Random index (RI) values for n factors (Saaty, 1977) .....**Error! Bookmark not defined.**

Table 3. Pairwise comparison matrices, factor weights, and consistency ratios from four expert participants, including consolidated values and consensus score 12

Table 4. Pairwise comparison matrices, normalized eigenvalue, consistency ratios and weighted overlay score of subclasses under each factor 14

Table 5. Groundwater potential zone categories and their respective composition 25

Table 6. AHP consensus indicator (Goepel, 2013 cited in Fildes et al., 2020) 29

1. INTRODUCTION

The Earth's surface is about 71% water, but only 2.5% of that is usable freshwater, a critical natural resource for supporting life, ecological systems and economic activity. Of this limited freshwater resource, roughly 68.7% is locked in glaciers and ice caps, around 30.1% lies beneath the surface as groundwater, and just 1.2% is accessible on the surface in rivers, lakes, and streams (Shiklomanov, 1993). Global freshwater consumption has shown a steady annual growth rate of approximately 1% over the past four decades, mainly driven by population growth, rapid urbanization, industrialization, agricultural intensification, forest degradation, and shifting consumption patterns, and this trend is expected to continue (UN, 2024, Gyeltshen et al., 2023). Natural and man-made surface water sources, including rivers, lakes, and reservoirs are becoming increasingly susceptible to seasonal fluctuations, overuse, and climate-induced stressors, while water sources are drying up across the globe, with the problem acutely felt in sensitive mountain regions like the Himalayas, where glacial retreat, shifting rainfall, and limited storage intensify water insecurity (Gyeltshen et al., 2023, Thapa et al., 2022, WMD, 2021). As a result, groundwater, the planet’s largest source of freely available liquid freshwater, is increasingly recognized as a vital and dependable resource due to its widespread availability, relative stability, and resilience to short-term climate variability (Rani et al., 2022, Saranya and Saravanan, 2020, Pirasteh et al., 2025). Globally, approximately 70% of withdrawn groundwater is used in agriculture and contributes to nearly 50% of the world’s drinking water supply (NGWA, 2024). Its role is particularly critical in arid to semi-arid regions, where surface water resources are inadequate or unpredictable (Gyeltshen et al., 2023). In South Asia, groundwater plays a dominant role in sustaining agriculture and rural livelihoods. In India, for example, around 60% of irrigation requirements are met through groundwater abstraction, and nearly 85% of rural communities rely on it as their main water source (Shelar et al., 2023).

In Bhutan, despite the abundance of surface water, estimated at approximately 94,500 cubic meters per person annually, the country is facing increasing water stress, particularly during the dry seasons (NEC, 2016, WMD, 2021). Bhutan's mountainous topography makes the development of delivery infrastructure difficult and limited in many rural communities (Tariq et al., 2021). Moreover, the reliability of surface water is declining due to the drying up of sources caused by changing climate patterns and land use transformations, while projected climate variability is expected to introduce further uncertainties (WMD, 2021, NCHM, 2024). According to the Watershed Management Division (WMD) 2021 report, 0.9% of the 7,399 assessed surface

drinking water sources in Bhutan have already dried up, and with 25.1% of surface water sources in the process of drying up, groundwater is emerging as a crucial alternative.

Groundwater potential is the ability of an area to store and yield usable groundwater (Arulbalaji et al., 2019). It is determined by interaction of several physical processes, including the movement of water from higher to lower elevations, its accumulation in low-lying areas and infiltration through permeable surfaces. These processes are influenced by a combination of hydrogeological, climatic, and geomorphological variables such as the permeability and porosity of geological formations, the amount and distribution of rainfall, ambient temperature affecting recharge and evaporation, slope angle and terrain height that govern runoff and infiltration, wetness index and drainage patterns indicating moisture accumulation, land use land cover that influence infiltration and evapotranspiration, and linear geological features such as faults and lineaments that can enhance groundwater flow and recharge (Rani et al., 2022, Sarkar et al., 2022, Gyeltshen et al., 2023, Gupta et al., 2022). While traditional methods of groundwater exploration, including drilling and geophysical surveys and electrical resistivity tomography (ERT) remain effective, they are often resource-intensive and time-consuming (Maizi et al., 2023, Lentswe and Molwalefhe, 2020, DGM, 2022). On the other hand, statistical and machine learning approaches such as boosted regression trees (BRT), random forests (RF), and classification and regression trees (CART) along with performance comparisons using bivariate methods like the evidential belief function (EBF) and multivariate models such as the general linear model (GLM), offer advanced alternatives for assessing groundwater potential by analysing the spatial relationships between known groundwater occurrences and multiple environmental factors, but these methods are often complex and require large, high-quality datasets such as groundwater data (Díaz-Alcaide and Martínez-Santos, 2019). In absence of such datasets, multi-criteria decision analysis (MCDA), particularly the analytical hierarchy process (AHP) integrated with geographic information systems (GIS) and remote sensing (RS) is knowledge-based, offering scalable, rapid, and cost-effective alternatives for groundwater potential mapping and site suitability analysis (Moumane et al., 2025). Globally, this methodology has been widely used to identify areas with high groundwater potential across a range of hydrogeological settings (Díaz-Alcaide and Martínez-Santos, 2019, Sarkar et al., 2022, Arulbalaji et al., 2019).

Although groundwater is not extensively utilized in Bhutan, limited abstraction does occur at the household level in valleys of some districts (Tariq et al., 2021). Comprehensive scientific studies on groundwater remain sparse, largely due to lack of capacity and the prevailing belief that Bhutan's rugged terrain limits groundwater availability (Tariq et al., 2021). The National Integrated

Water Resources Management Plan (2016) highlights that very little is known about the country's groundwater resources, and their extent remains largely unassessed (NEC, 2016). Nevertheless, a few localized groundwater studies in Thimphu and Phuentsholing municipalities have facilitated evidence-based decisions in municipal water resource management by identifying potential groundwater zones, assessing aquifer characteristics such as yield and seasonal variations in water availability, thereby contributing to improved planning for water supply augmentation and reduced reliance on surface water sources (Thapa et al., 2022, Thongley et al., 2023, Gyeltshen et al., 2023). Additionally, a preliminary electrical resistivity tomography (ERT) study, conducted in 2022 in Gelephu, Sarpang District, provides initial insights into subsurface water potential, identifying saturated zones at varying depths in two locations, while no significant detection was made in the third (DGM, 2022).

Sarpang District, situated in south-central Bhutan, exemplifies a region facing emerging water shortage challenges. The Assessment and Mapping of Water Sources in Bhutan (2021) reports that 47.5% of surface water sources in Sarpang District are drying up (WMD, 2021). Although the region receives abundant rainfall and is traversed by many rivers and streams during the monsoon, residents face flooding in the wet season and severe water shortages during the dry months (DAS, 2018). The current population of Sarpang is 48,095 people (NSB, 2017). Notably, none of Bhutan's major river systems flow through the district, further increasing its vulnerability to water scarcity. This challenge is compounded by the planned Gelephu Mindfulness City, which will span 2,600 km^2, encompassing the entire Sarpang District and parts of two adjacent districts, and is expected to accommodate approximately 1.2 million people in the coming decades (GMC, 2024). Furthermore, the city's development will be centred around seven core economic areas: spirituality, health and wellness, education and knowledge, green energy and technology sectors, finance, agri-tech and forestry, and the airport economy (GMC, 2024).

Apart from the limited ERT study conducted in three areas of Gelephu, no comprehensive groundwater studies have been undertaken in the district. As the region faces growing water shortages driven by climate variability, increasing demand, and the decline of surface water sources, groundwater exploration and management have become critical. This study seeks to address these gaps by assessing where the most promising groundwater potential zones are located. Using multi-criteria decision analysis (MDCA) approach, integrating GIS, RS and the AHP. GIS enables spatial analysis and data integration and RS supplies key datasets like land cover and terrain, while AHP provides a systematic approach to weighting the importance of each factor. The study incorporates parameters such as geology, slope, soil type, rainfall, land use land cover,

drainage, and lineament density to produce a groundwater potential map. These findings will offer an evidence-based foundation for sustainable groundwater exploration, strategic planning, and efficient water resources management. In particular, the study supports the long-term water security needs of large-scale developments like the Gelephu Mindfulness City by identifying viable groundwater sources that can complement surface water systems, ensuring a resilient and reliable water supply for future urban growth.

2. STUDY AREA

2.1. Location

Located in south-central Bhutan, Sarpang District, the study area, extends between 26°51'50.22"N latitude and 90°16'2.82"E longitude. It covers an area of approximately 1,655 km^2 and lies within the 2,500 km^2 designated for the Gelephu Mindfulness City. Sarpang exhibits significant altitudinal variation, ranging from 168 meters to 4,199 meters above sea level (Figure 1). This substantial topographic range gives rise to diverse ecological zones, microclimates, and temperature gradients across the district (DGM, 2022, DAS, 2018).

Figure removed due to copyright restriction.

Figure 1. A comprehensive map of the Sarpang district study area, generated using the SRTM Global Digital Elevation Model (DEM).

2.2. Climate and hydrology

Southern foothills experience hot and humid summers, with annual average temperatures often exceeding 30°C, while the northern highlands are considerably cooler, with winter temperatures occasionally falling as low as 13°C (DAS, 2018). The district experiences a prolonged subtropical

monsoon weather marked by distinct wet and dry seasons, with rainfall usually beginning in May and continuing through September, while October to March remain relatively dry (Figure 2 b). Annual precipitation ranges from 1,000 mm to 4,199 mm, generally decreasing from the southern lowlands to the northern highlands (DAS, 2018). Several rivers and streams, along with numerous tributaries, drain Sarpang, most notably the Mao Khola and Taklai Rivers. A large number of these streams are seasonal in nature and commonly experience drying periods throughout the winter months (WMD, 2021). However, none of Bhutan's major river systems flow through the district.

Figure removed due to copyright restriction.

Figure removed due to copyright restriction.

Figure 2: (a) Monthly average minimum and maximum temperatures, and (b) monthly and annual rainfall from 1996 to 2024, recorded at the Bhur Weather Station. Data source: National Centre for Hydrology and Meteorology (NCHM, 2024).

3. MATERIAL AND SOURCES

This study used a range of spatial and thematic datasets to estimate and locate groundwater potential areas in Sarpang District, Bhutan. ArcGIS Pro 3.4.0 was the primary software used for processing thematic layers and data in this study.

Sarpang district, sub-block maps and river maps: The district and sub-block administrative maps and river maps were obtained from the National Land Commission, Royal Government of Bhutan.

Digital Elevation Model (DEM): A 30m resolution Shuttle Radar Topography Mission (SRTM) 1 Arc-Second Global DEM was acquired from the USGS Earth Explorer platform (USGS, 2014). The DEM was processed in GIS to derive three topographic parameters - slope, lineament density, and drainage density.

Rainfall map and data: Rainfall data processing involved two data sources: local rainfall data from 1996 to 2024 retained with the National Centre for Hydrology and Meteorology (NCHM), Bhutan for spatial validation and long-term rainfall data map from WorldClim version 2.1 climate dataset (Fick, 2017).

Soil map: Soil type map was prepared using the 1:250,000 scale soil map of Bhutan obtained from the National Soil Service Centre (NSSC) under the Department of Agriculture, Ministry of Agriculture and Livestock, Bhutan.

Geology map: A 1:500,000 scale geologic map of Bhutan prepared by Long et al. (2011), was sourced in Keyhole Mark-up Language zipped format (kmz) from Department of Geology and Mines, Ministry of Energy and Natural Resources, Bhutan for the geologic thematic map.

Land Use and Land Cover (LULC) map: The 10m resolution LULC map of Bhutan 2016 was obtained from National Land Commission Secretariat (NLCS), Bhutan, and was used in preparing LULC as one of the thematic maps influencing the groundwater recharge.

4. METHODOLOGY

The methodology consists of four main components: selection of groundwater-influencing factors, preparation of thematic layers, application of the AHP to derive factor weights, and final mapping of groundwater potential zones (GPZs) using the weighted overlay analysis (WOA) method. While AHP provides a structural framework for determining the relative importance of each factor, it is the WOA method that integrates these weighted layers to generate the final GPZ map.

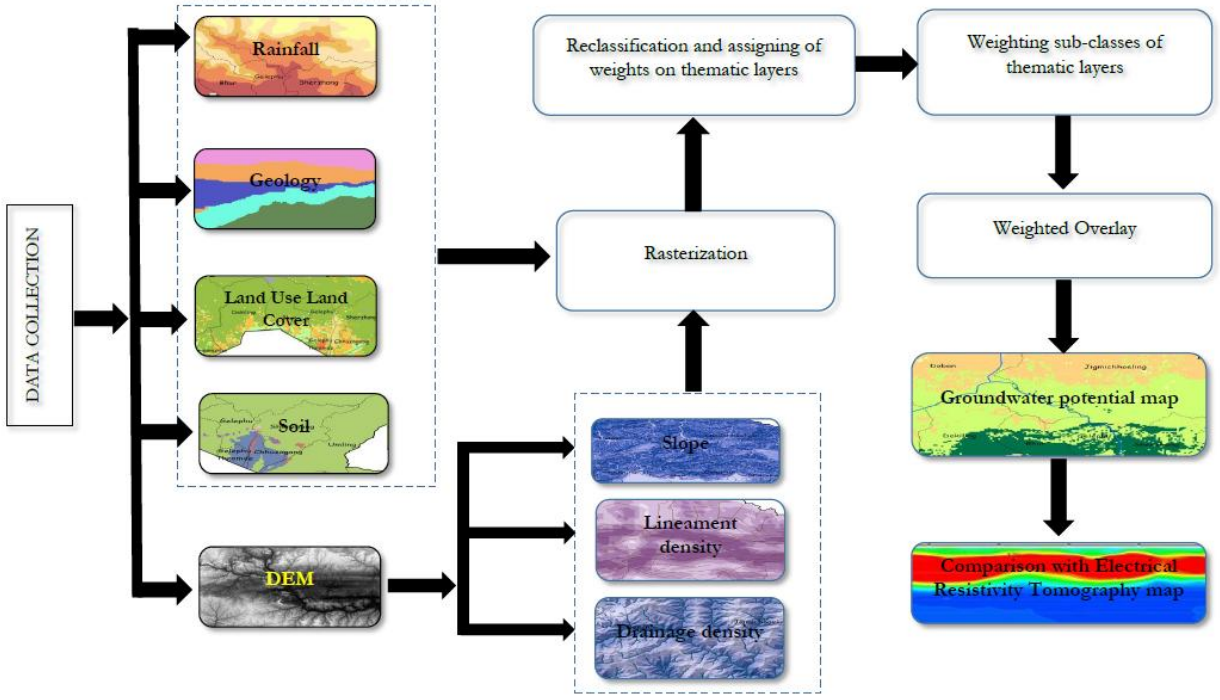

Figure 3: Overview of the methodology used for groundwater potential mapping.

4.1. Selection of groundwater-influencing factors

Groundwater recharge is governed by a complex interplay of factors, including soil type, geological and lithological characteristics, rainfall distribution, LULC, slope gradient, drainage patterns, lineament density, geomorphology, and proximity to rivers, among others (Díaz-Alcaide and Martínez-Santos, 2019, Atalla et al., 2024, Derdour et al., 2022). Findings from studies using the multi-influencing factor, analytical hierarchy process, and frequency ratio methods indicate that lithology, rainfall, soil type, and lineament density are the most influential factors in determining groundwater potential (Ahmed et al., 2021). Fildes et al. (2020) classify groundwater-influencing factors into three categories based on their function: rainfall and aspect fall under the ‘supply’

category; lithology and lineaments represent ‘infiltration pathways’**;** and slope and the topographic wetness index belong to the **‘**opportunity’ group (Fildes et al., 2020). Based on the review of the selected literature, as summarized in Figure 3, this study assumes that factors more frequently cited, such as geology, lineament density, drainage density, rainfall, land use land cover, slope and soil type, exert a stronger influence on groundwater recharge process, and thus have been selected for their consistent relevance and demonstrated impact on groundwater potential mapping.

All thematic layers were projected to the DRUKREF 03 Bhutan National Grid coordinate system and resampled to a spatial resolution of 100 m by 100 m.

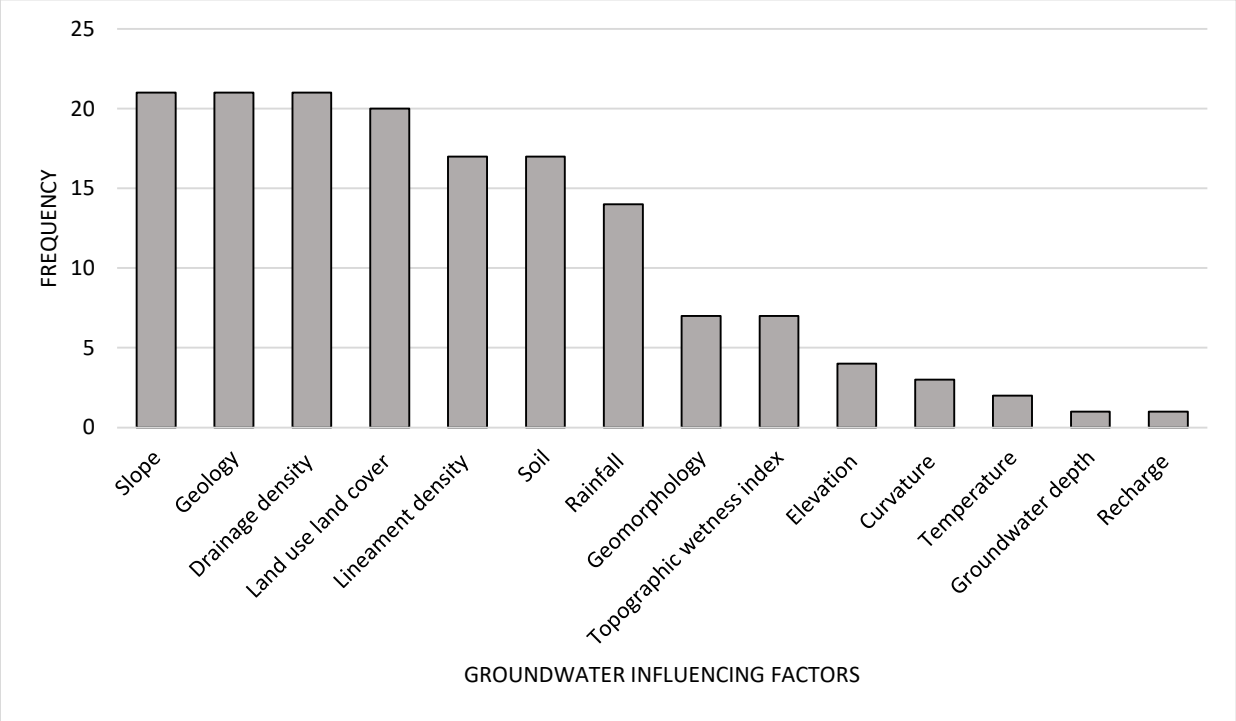

Figure 4: Frequency of groundwater influencing factors used for 21 groundwater potential studies conducted in sub-Indian continent and African countries, using GIS, RS and AHP.

4.2. Application of Analytical Hierarchy Process

Groundwater potential mapping involves evaluating the relative importance of multiple spatial and thematic factors that influence groundwater occurrence and recharge, providing the basis for applying the AHP to assign weights to each factor. The Analytical Hierarchy Process (AHP) effectively aids decision-makers in handling complex, conflicting, and subjective criteria, and when integrated with GIS and remote sensing (RS), AHP facilitates the delineation of groundwater

potential zones by weighting and overlaying thematic layers (Ishizaka and Labib, 2009, Beden et al., 2023). In the AHP method, groundwater-influencing factors are assigned weights based on their relative importance using a scale from 1 to 9, as shown in Table 1. The procedure includes preparing a pairwise comparison matrix, normalizing it, calculating normalized weights, deriving the weighted sum vector for feature eigenvalue estimation, computing the principal eigenvalue, and then determining the consistency index and consistency ratio using Saaty's random index as shown in Table 2.

Table 1. A numerical scale used for pairwise comparisons in AHP (Saaty, 1977)

Intensity of importance	Definition	Explanation
1	Equal importance	Two elements contribute equally to the objective
3	Moderate importance	Experience and judgment slightly favour one element over another
5	Strong Importance	Experience and judgment strongly favour one element over another
7	Very strong importance	One element favoured very strongly over another, it dominance is demonstrated in practice
9	Extreme importance	The evidence favouring one element over another is of the highest possible order of affirmation
2,4,6,8 are intermediate values between two adjacent judgments when compromise is needed		

Table 2. Random index (RI) values for n factors (Saaty, 1977)

n	1	2	3	4	5	6	7	8	9	10	11
RI	0	0	0.58	0.9	1.12	1.24	1.32	1.41	1.45	1.49	1.51

In the pairwise comparison process, each thematic factor is compared with others using a scale of 1 to 9 to reflect its relative importance, forming a matrix essential for calculating the normalized principal eigenvector that represents the parameter weights (Saaty, 1977, Homtong et al., 2024). In this study, expert judgments from four individuals, a hydrologist, a geospatial scientist and two environmentalists, were used to construct the pairwise comparison matrix, calculate eigenvalues, and assess consistency using Goepel's row geometric mean method through an online AHP calculator and excel worksheet (Goepel, 2018). Table 3 presents the pairwise comparison

matrices, eigenvalue-derived weights, and consistency ratios for individual experts' scores, alongside the consolidated matrix and its corresponding eigenvalue weights.

To normalize the matrix, the sum of each column is first calculated. Then, each element in the pairwise comparison matrix is divided by the total of its respective column, using Eq. (1).

$$\text{Normalized matrix value} = \frac{Aij}{\text{Column sum of } j} \quad (1)$$

A is pair comparison matrix, i = row index and j = column index

Next, the weight assigned to each factor is obtained by calculating the average of the normalized values across its respective row, as illustrated in Equation (2).

$$\text{Normalized Weight (w)} = \sum_{j=1}^{n} \frac{\text{Normalized matrix(ij)}}{n} \quad (2)$$

n= number of factors

Eq. (3) is used to derive the weighted sum vector (Aw), achieved by multiplying the pairwise comparison matrix with the corresponding normalized weight vector (w). This calculation indicates the contribution of each criterion to the overall priority.

$$\text{Weighted sum vector (Aw)} = \sum_{j=1}^{n} Aij \times wj \quad (3)$$

To calculate the average principal eigenvalue (λ), the eigenvalue for each factor is first computed using Eq. (4), and the average of these values, obtained using Eq. (5), represents the principal eigenvalue.

$$\text{Eigenvalue for each factor } \lambda i = \frac{Aw\ (i)}{w(i)} \quad (4)$$

$$\text{Principal Eigenvalue } (\lambda max) = \frac{\Sigma \lambda i}{n} \quad (5)$$

In AHP, the Consistency Ratio (CR) plays an important role in verifying whether the weights derived from the pairwise comparison matrix are logically inconsistent, an essential aspect of the methodology (Fildes et al., 2020). Eq. (6) is used to compute the Consistency Ratio (CR), with 0.1 (10%) defined by Saaty as the upper limit for acceptable consistency (Homtong et al., 2024).

$$\text{Consistency Ratio (CR)} = \frac{\text{CI}}{\text{RI}} \quad (6)$$

Consistency index (CI) is calculated using Eq. (7) and random index (RI) is derived from Saaty's RI values, which is 1.32 for 7 factors from Table 2.

$$\text{Consistency index (CI)} = \frac{\lambda_{\text{max-n}}}{\text{n -1}} \quad (7)$$

As shown in Table 3, geology has the highest contribution at 29%, followed by lineament density at 20%. The least contributing factor, based on the consolidated matrix, is land use land cover, contributing only 6%.

Table 3. Pairwise comparison matrices, factor weights, and consistency ratios from four expert participants, including consolidated values and consensus score

SN	Influencing factor	1	2	3	4	5	6	7	Normalized eigenvalue (w)
	Expert 1 (E-1)								
1	Geology	1	1	3	3	3	6	7	0.289
2	Lineament density	1	1	3	4	5	5	6	0.312
3	Slope	1/3	1/3	1	1	2	2	4	0.115
4	Rainfall	1/3	1/4	1	1	1	2	5	0.105
5	Drainage density	1/3	1/5	1/2	1	1	2	4	0.090
6	Soil	1/6	1/5	1/2	1/2	1/2	1	3	0.059
7	Land use land cover	1/7	1/6	1/4	1/5	1/4	1/3	1	0.030
	Consistency ratio = 0.026								
	Expert 2 (E-2)								
1	Geology	1	1	4	4	4	5	7	0.307
2	Lineament density	1	1	4	4	4	5	7	0.307
3	Slope	1/4	1/4	1	1	1	3	5	0.104
4	Rainfall	1/4	1/4	1	1	1	3	5	0.104
5	Drainage density	1/4	1/4	1	1	1	3	4	0.099
6	Soil	1/5	1/5	1/3	1/3	1/3	1	3	0.051
7	Land use land cover	1/7	1/7	1/5	1/5	1/4	1/3	1	0.028
	Consistency ratio = 0.033								

	Expert 3 (E-3)									
1	Geology	1	5	3	1/7	3	1/4	1/4	0.089	
2	Lineament density	1/5	1	1/2	1/8	1/4	1/5	1/7	0.027	
3	Slope	1/3	2	1	1/8	1/2	1/5	1/7	0.037	
4	Rainfall	7	8	8	1	8	4	5	0.435	
5	Drainage density	1/3	4	2	1/8	1	1/6	1/6	0.053	
6	Soil	4	5	5	1/4	6	1	2	0.195	
7	Land use land cover	2	7	7	1/5	6	1/2	1	0.165	
	Consistency ratio= 0.085									
	Expert 4 (E-4)									
1	Geology	1	2	1/2	1/4	3	1/2	3	0.112	
2	Lineament density	1/2	1	1/3	1/7	1/3	1/2	2	0.056	
3	Slope	2	3	1	1/3	4	4	2	0.193	
4	Rainfall	4	7	3	1	6	5	7	0.412	
5	Drainage density	1/3	3	1/4	1/6	1	1/2	1	0.067	
6	Soil	2	2	1/4	1/5	2	1	2	0.107	
7	Land use land cover	1/3	1/2	1/2	1/7	1	1/2	1	0.052	
	Consistency ratio = 0.068									
	Consolidated								Eigenvalue and percentage	
1	Geology	1	1 7/9	3 1/2	1 4/5	4	2 1/2	3 3/4	0.292	29
2	Lineament density	5/9	1	2	1 7/9	2 1/3	2 1/9	2 5/9	0.198	20
3	Slope	2/7	1/2	1	7/9	1 2/5	1 1/4	2	0.107	11
4	Rainfall	5/9	5/9	1 2/7	1	2	1 6/7	4 2/5	0.164	16
5	Drainage density	1/4	3/7	5/7	1/2	1	3/4	1 1/2	0.078	8
6	Soil	2/5	1/2	4/5	1/2	1 1/3	1	3	0.106	10
7	Land use land cover	1/4	2/5	1/2	2/9	2/3	1/3	1	0.055	6
	Consistency ratio = 0.017									
	Expert consensus score = 55.8%									

Each influencing factor includes sub-classes that vary in their impact on groundwater potential. Each factor was further divided into five sub-categories, ranked on a scale from 1 to 5, where 5 indicates the highest and 1 the lowest contribution based on their characteristics related to groundwater potential. As shown in Table 4, pairwise comparison matrices, normalization matrices, normalized eigenvalues, consistency indices, and consistency ratios were calculated for the sub-classes of each factor using the Goepel's (2013) online AHP calculator.

Table 4. Pairwise comparison matrices, normalized eigenvalue, consistency ratios and weighted overlay score of subclasses under each factor

Influencing features	Normalized eigenvalue (w)	Subclasses	1	2	3	4	5	Normalized eigenvalue (wi)	AHP weighted overlay contribution scale (from 1-5)
Geology	0.292	(1) Quaternary sediments	1	3	4	5	6	0.416	5
		(2) Buxa-Tethyan group (Ordivician)	1/3	1	3	4	5	0.262	4
		(3) Sub-Himalayan zone (Miocene-Pliocene)	1/4	1/3	1	3	4	0.161	3
		(4) Greater Himalayan zone (Neoprotezoroic-Ordovician)	1/5	1/4	1/3	1	2	0.099	2
		(5) Buxa Group-Daling formation (Paleoprotezoroic)	1/6	1/5	1/4	1/2	1	0.062	1
		Consistency ratio: 0.055							
Lineament density (km/sq.km)	0.198	(1) > 5	1	2	3	4	5	0.416	5
		(2) 4 - 5	1/2	1	2	3	4	0.262	4
		(3) 3 - 4	1/3	1/2	1	2	3	0.161	3
		(4) 2 - 3	1/4	1/3	1/2	1	2	0.099	2
		(5) < 2	1/5	1/4	1/3	1/2	1	0.062	1
		Consistency ratio: 0.015							
Slope (degrees)	0.107	(1) < 5	1	3	5	7	9	0.505	5
		(2) 5 - 15	1/3	1	3	5	6	0.254	4
		(3) 15 - 25	1/5	1/3	1	3	5	0.136	3
		(4) 25 - 35	1/7	1/5	1/3	1	3	0.069	2
		(5) > 35	1/9	1/6	1/5	1/3	1	0.036	1
		Consistency ratio: 0.055							
Rainfall (mm)	0.164	(1) > 3600	1	2	3	4	6	0.423	5
		(2) 2901 - 3600	1/2	1	2	3	5	0.269	4
		(3) 2300 - 2900	1/3	1/2	1	2	3	0.157	3

		(4) 1801 - 2300	1/4	1/3	1/2	1	2	0.096	2
		(5) < 1800	1/6	1/5	1/3	1/2	1	0.055	1
		Consistency ratio: 0.01							
Drainage density (km/sq.km)	0.078	(1) < 1	1	2	3	4	5	0.416	5
		(2) 1 - 2	1/2	1	2	3	4	0.262	4
		(3) 2 - 3	1/3	1/2	1	2	3	0.161	3
		(4) 3 - 4	1/4	1/3	1/2	1	2	0.099	2
		(5) > 4	1/5	1/4	1/3	1/2	1	0.062	1
		Consistency ratio: 0.015							
Soil types	0.106	(1) Eutric cambisols	1	2	3	4	5	0.416	5
		(2) Dystric cambisols	1/2	1	2	3	4	0.262	4
		(3) Haplic cambisols	1/3	1/2	1	2	3	0.161	3
		(4) Athraquic cambisols	1/4	1/3	1/2	1	2	0.099	2
		(5) Skeletic cambisols	1/5	1/4	1/3	1/2	1	0.062	1
		Consistency ratio: 0.015							
Land use land cover	0.055	(1) Water bodies	1	2	5	7	9	0.464	5
		(2) Forest and meadows	1/2	1	3	5	8	0.284	4
		(3) Shrubs and cultivated agriculture	1/5	1/3	1	3	7	0.143	3
		(4) Alpine and non-built up areas	1/7	1/5	1/3	1	5	0.078	2
		(5) Landslides, built-ups and rocky outcrops	1/9	1/8	1/7	1/5	1	0.031	1
		Consistency ratio: 0.073							

4.3. Weighted overlay analysis

A Groundwater Potential Suitability Index was developed using the 'Weighted Overlay Analysis' tool to generate the groundwater potential zone map. This method integrates the contributions of seven selected influencing variables, each weighted according to their relative importance derived from the AHP pairwise comparison matrices (Table 3). Within each factor, sub-classes were assigned scaled weights from 1 to 5 based on their influence on groundwater potential (Table 4). The final index combines the weighted influence of each factor and its sub-classes, as shown in Eq. (8).

$$GP = RfwRfwi + SlwSlwi + LULCwLULCwi + SwSwi + GwGwi + DDwDDwi + LDwLDwi \quad (8)$$

Where, the thematic layers are Rainfall (Rf), Slope (Sl), Land Use Land Cover (LULC), Soil (S), Geology (G), Drainage Density (DD), and Lineament Density (LD). The normalized weight assigned to each thematic layer is denoted by 'w' (Table 3), while 'wi' represents the normalized weight of the sub-classes within each layer (Table 4).

5. RESULTS AND DISCUSSION

5.1. Geology

The lithology and structural geology of the region play a critical role and are the most significant factors in defining groundwater potential, as they govern subsurface water movement through various rock types, structural features, and formation boundaries identified in geological maps (Díaz-Alcaide and Martínez-Santos, 2019, Adama et al., 2024, Sarkar et al., 2022). The geologic map, derived from the 1:500,000 Geological map of Bhutan by Long et al. (2011), reveals a range of distinct geological formations (Figure 5). Quaternary sediments found in the study area are unconsolidated sediments consisting of rounded pebbles to boulders in clayey-sandy matrices, often forming terraces and fans in foothills and valleys (Bharga, 1995). Although it is known to have a high positive influence on groundwater recharge, its spatial extent in the area is limited. Sub-Himalayan Siwalik (Miocene-Pliocene) formations in the south-east flood plains form 2.8% of the area and are correlated with clay and tan to grey coarse-grained and conglomeratic sandstone, which have moderate groundwater recharge factor, particularly the porous sandstone (Bharga, 1995, Gyeltshen et al., 2023). Bharga (1995) describes the Buxa group (Neoproterozoic–Cambrian covers 38.9% of the area) as a geology group with varying thicknesses of limestone, dolomite, quartzite and shale, and Thapa et al. (2022) describe it as highly fractured schists, slates, and phyllites. While, dolomite and limestone with karst fractures and highly fractured schist favour groundwater infiltration, quartzite and shale are known for their impermeability (Gyeltshen et al., 2020, Gyeltshen et al., 2023, Thapa et al., 2022). Lithology for Daling-Shumar (Paleoproterozoic) formation group covering 8% is described to predominantly have green phyllite and schist fine-grained quartzite inter-beds, which is favourable for water infiltration (Bharga, 1995, Thapa et al., 2022, Gyeltshen et al., 2023, NSSC, 2024). The Greater Himalayan Zone (Neoproterozoic–Ordovician and Cambrian–Ordovician), which is still under research (Long et al., 2011), constitutes a substantial section of the area, covering 49.5% of the central and northern regions. It is characterized by weathering, granitic orthogneiss composition, and abundant feldspar, all of which have varying influences on groundwater recharge (Thapa et al., 2022).

Each geological subclass is weighted according to its respective role in affecting groundwater availability (Table 4).

Figure removed due to copyright restriction.

Figure 5: Geological features of the study area, adapted from Long et al. (2011).

5.2. Lineament density

Lineaments, which are surface expressions of faults or fractures often visible as straight alignments in satellite imagery, play a vital role with higher secondary porosity and permeability, thereby facilitating groundwater movement and recharge (Gupta et al., 2022, Shelar et al., 2023, Fildes et al., 2025). The lineaments were derived from 1:500,000 geologic map and DEM-derived hill-shades with the different (90-60, 150-30, 50-90, 100-60, 200 50, 315-45) Azimuth-Altitude combinations. The lines created were further processed into lineament density (LD) using the line density tool of GIS. The LD is the total kilometre of lineaments per square kilometre using Eq. (9) within 100 m x 100 m resolution, consistent with other factors.

$$\text{Lineament density (LD)} = \frac{\text{Total length of lineament in a unit area (km)}}{\text{Area of the unit (km2)}} \quad (9)$$

Regions exhibiting greater lineament density are regarded as more conducive to groundwater recharge and are therefore assigned higher priority in the AHP weighting process (Gupta et al., 2022). The LD values have been classified into five scale categories (1-5) using the Natural Breaks (Jenks) optimization method.

Figure removed due to copyright restriction.

Figure 6: Lineament and lineament density map derived from 30m resolution SRTM 1 Arc-Second Global DEM.

5.3. Slope

Slope affects the rate of infiltration and the pattern of surface runoff, which in turn influences groundwater recharge. Steeper slopes promote rapid surface runoff and hinder infiltration, while flatter and gentler terrains facilitate higher infiltration rates, enhancing groundwater recharge (Atalla et al., 2024). A slope map derived from a 30 m DEM using slope analysis tools in GIS ranges from flat to very steep with a maximum of 35 degrees. Most of the southern belt and river valleys range from flat to very gentle, while the central and northern parts are mostly steep terrain. Flatter slopes generally promote infiltration and receive higher ranking in the AHP process, while

steeper areas contribute more to surface runoff and are assigned lower weights. The slope layer was resampled into standard 100 m x 100 m resolution for weighted overlay.

Figure removed due to copyright restriction.

Figure 7: Slope map based on 30 m resolution SRTM 1 Arc-Second Global DEM.

5.4. Rainfall

Rainfall is widely recognized as one of the most significant hydrological factors contributing to groundwater, as it directly determines the amount of available water for infiltration into the subsurface (Maizi et al., 2023, Adama et al., 2024, Mukherjee et al., 2012). A long-term annual rainfall data map obtained from WorldClim version 2.1 with rainfall data records from 1970-2000 (Fick, 2017), was processed within the study area using the GIS spatial analyst tool. The map is classified into different rainfall zones consistent with other factors, each representing varying levels of groundwater recharge potential. As evident from Figure 8, the south-east region receives higher annual rainfall (not less than 3500 mm) while the northern parts receive less annual rainfall (below 1800 mm). Different rainfall zones are assigned different weights in AHP, and high rainfall zones are assigned with higher weights as they contribute more to recharge. The classified map is resampled to 100 m x 100 m resolution for overlay weighting.

Figure removed due to copyright restriction.

Figure 8: Sarpang district rainfall map derived from WorldClim version 2.1 climate with dataset from 1970-2000.

5.5. Drainage density

Drainage density (DD) quantifies how closely spaced the drainage networks are in a particular area, expressed as the total drainage length per unit area, which inversely affects groundwater recharge. Low drainage density areas, indicative of higher infiltration and lower runoff, are ranked higher in AHP and conversely, high drainage density areas suggest poor recharge conditions due to lower infiltration from more runoff (Mukherjee et al., 2012). It is derived from hydrological analysis of a DEM by using series of GIS tools: filling for hydrological correction, creating flow direction and accumulation, generating drainage network and stream order. The DD is calculated as total drainage length per unit area using Eq. (10).

$$\text{Drainage density (DD)} = \frac{\text{Total length of drainage in a unit area (km)}}{\text{Area of the unit (km2)}} \quad (10)$$

The DD map is classified into 5 categories using the Natural Breaks (Jenks) optimization method, which determines the weights in AHP overlay weight analysis.

Figure removed due to copyright restriction.

Figure 9: Drainage network and drainage density map of Sarpang district derived from SRTM 1 Arc-Second Global DEM.

5.6. Soil

Soil type significantly influences groundwater recharge by determining how effectively water infiltrates into the subsurface, largely based on the soil's permeability and its capacity to retain moisture, with sandy loam exhibiting high infiltration rates and good groundwater potential, while clay has low infiltration rates and limited groundwater potential (Lentswe and Molwalefhe, 2020, Saranya and Saravanan, 2020, Phoemphon and Terakulsatit, 2023). The study area soil map was processed from the Bhutan Soil Map, obtained from the National Soil Protection and Service Centre, 2024 Bhutan. The soil map has the following soil types - Dystric Cambisols, Eutric Cambisols, Anthraquic Cambisols, Skeletic Cambisols, and Haplic Acrisols. They have varying implications on infiltration, recharge, and storage capacity (NSSC, 2024). The predominant soil type in the study region is Cambisols, which generally have high clay and silt content, resulting in

low permeability and high water retention that can limit groundwater recharge (Ružičić et al., 2019). Among these, Dystric Cambisols are the most widespread, covering 93% of the study area, followed by Eutric and Anthraquic Cambisols, with minor occurrences of Skeletic Cambisols.

Figure removed due to copyright restriction.

Figure 10: Soil types of the study area, Sarpang district (NSSC, 2024).

5.7. Land use - land cover

Land use and land cover (LULC) directly influence water recharge, evapotranspiration, and runoff, thereby affecting the infiltration and groundwater recharge capacity of a watershed or sub-basin. LULC data also provide essential information on soil moisture, surface water, groundwater, and serve as indicators for groundwater potential development (Homtong et al., 2024, Phoemphon and Terakulsatit, 2023). In the study area, as shown in Figure 11, forests dominate the landscape, covering 1,484 km² or 90 % of the total area. Forested regions play a crucial role in groundwater recharge, as vegetative cover significantly influences actual recharge rates (DWLBC, 2002). (Hümann et al., 2011) note that “soils under natural forests tend to be relatively porous with high

infiltration rates, which lowers the rates of surface runoff." Cultivated agricultural land occupies 81 km², representing 5 % of the study area. Such lands can be favorable for recharge depending on soil type, crop type, and irrigation practices (Murphy et al., 2021). The study area also contains minor proportions of other LULC categories: shrubs (3 %), meadows, water bodies, built-up areas, non-built-up areas, alpine scrubs, and rocky outcrops, all of which exert varying degrees of influence on groundwater recharge.

Figure removed due to copyright restriction.

Figure 11: Land use - land cover types of Sarpang district derived from LULC map of NLCS, 2016.

5.8. Groundwater potential map

The Groundwater Potential Zone (GPZ) map for Sarpang District, developed using AHP, categorizes the extensive study area into three zones: High, Moderate, and Low Potential as shown in Figure 12.

Figure removed due to copyright restriction.

Figure 12: Groundwater potential map of Sarpang district categorized into three zones based on 55.8% consensus weights scoring from four expert participants.

Table 5. Groundwater potential zone categories and their respective composition

Area (sq.km)	Percentage	Groundwater potential
445	28	Low
795	51	Moderate
327	21	High

From Table 5, the high groundwater potential zone covers approximately 327 square kilometres, representing 21 % of the total study area. These zones are primarily spread at the southern border, mainly concentrated within south-central plains as shown in Figure 12. Except for lower lineament density, the distribution corresponds to other favourable hydrogeological conditions such as flat topography and high rainfall (Figure 7 and 8). These factors have a strong positive

influence on groundwater recharge. The combination of high infiltration capacity and proximity to drainage networks in these regions further enhances groundwater recharge, making them highly suitable for groundwater development. The moderate potential zone occupies the largest study area, measuring 795 km^2, which is approximately 51% of the total area. This zone predominantly extends across the central parts of the district, which is characterized by gently sloping terrain and mixed land use (Figure 7 and 11). These areas offer relatively favourable conditions for groundwater occurrence, though not as optimal as the high-potential zones. The remaining 445 km^2, accounting for 28% of the study area, falls under the low groundwater potential zone, primarily located in the northern region. This area is characterized by steep slopes, rugged terrain, and low rainfall area, all of which limit groundwater recharge. These findings provide valuable information for strategic groundwater planning by identifying areas with higher groundwater potential, thereby supporting informed decision-making for sustainable water resource development.

5.9. Conformity with Electrical Resistivity Tomography test

Electrical Resistivity Tomography (ERT) is a geophysical method that generates high-resolution subsurface images by mapping variations in the electrical resistivity of rocks, minerals, and other materials (Torgashov, 2012). It is widely used in groundwater exploration to investigate and assess subsurface water resources (Norooz et al., 2024). In 2022, ERT surveys were conducted at three locations; Pelrithang, Dzomlingthang, and Lekithang within the Gelephu block of Sarpang District, investigating subsurface conditions to depths of approximately 40 to over 100 meters, with the depth to the water table inferred from sharp drops in resistivity values interpreted as saturated zones (DGM, 2022). As evident from Figure 13, at Pelrithang, a notable drop in resistivity values at around 40–50 meters depth was interpreted as a saturated zone, while at Dzomlingthang, a similar decline at around 20 meters indicated potential aquifer presence. In contrast, Lekithang exhibited limited low-resistivity zones and no clear evidence of saturation, suggesting the absence of significant groundwater-bearing formations.

Figure removed due to copyright restriction.

Figure removed due to copyright restriction.

Figure removed due to copyright restriction.

(c)

Figure 13: 3-D inversion results showing subsurface layers at (a) Pelrithang, (b) Dzomlingthang, and (c) Lekithang. Source: DGM (2022)

However, the report cautions that the resistivity values are inherently non-unique and can be influenced by various factors such as clay content, soil moisture, and compaction (DGM, 2022). As such, distinguishing between true aquifer zones and fine-grained, conductive materials remains challenging without supporting data such as borehole logs.

Furthermore, while Pelrithang and Dzomlingthang fall within the high groundwater potential zones identified by the AHP-based model, the spatial overlap should be interpreted with caution. The AHP method involves subjective weighting and relies on generalized datasets, which introduces uncertainty. Therefore, although there is general agreement between ERT results and AHP predictions in some areas, this convergence alone is not sufficient to confirm groundwater presence without ground-truthing.

Figure removed due to copyright restriction.

Figure 14: Comparison of Electrical Resistivity Tomography (ERT) test locations with AHP-derived groundwater potential zones.

6. UNCERTAINTY AND LIMITATIONS

A key component of the AHP is the assignment of weights to influencing factors. These weights are typically based on an individual's perceived importance of each factor in relation to the desired outcome (Fildes et al., 2020). However, Diaz-Alcaide and Martínez (2019) argue that this method of assigning weights based on personal judgment is fundamentally rudimentary, introducing a high degree of subjectivity and potential bias into the analysis. To mitigate this issue, an alternative approach involves consensus-based weighting, where multiple experts provide their judgments, and a consolidated weight is derived for the AHP analysis (Fildes et al., 2020). In this study, the consensus score was calculated using Goepel's (2018) AHP calculator, which quantifies the level of agreement among expert judgments. The resulting consensus score was 55.8%, which, according to Goepel's consensus indicator (see Table 6), is considered 'low consensus'. This low consensus score highlights the inherent anomaly and subjectivity in expert judgment when assigning weights.

Table 6. AHP consensus indicator (Goepel, 2013 cited in Fildes et al., 2020)

Indicator (%)	Consensus
≤ 50 %	Very low
50-65 %	Low
65-75%	Moderate
75-85 %	High
≥ 85 %	Very high

To assess scoring anomalies, groundwater potential (GWP) maps were generated using the individual AHP weights provided by each expert, as shown in Figure 15. The differences in weights assigned by individual experts resulted in distinct groundwater potential maps. When these individual maps are compared with the consensus-based map, notable variations become evident, highlighting the inherent uncertainty in expert judgment. Nevertheless, all four individual maps consistently identify the northern region as a low groundwater potential area, indicating a shared assessment despite variations in weighting.

Figure removed due to copyright restriction.

Figure 15: Groundwater potential zones generated using individual AHP scores (normalized eigenvalues in Table 3) from four experts (E-1, E-2, E-3, and E-4).

Another source of uncertainty in the AHP method stems from the assumption of independence among influencing factors during weight assignment, an oversimplification that excludes associated uncertainties and may misrepresent each factor's true influence on groundwater potential (Radulović et al., 2022). In reality, groundwater factors often interact in complex ways, where one can amplify or suppress another's influence, distorting the assigned weights. Additionally, both individual and collective judgement can introduce bias into the results. To address these limitations, studies have increasingly applied methods like multi-influencing factor (MIF) approach, which offer a systematic approach to parameter weighting by comparing parameters pairwise and assigning values based on their mutual influence on each other, while Fuzzy AHP accounts for uncertainty and variability in expert judgements (Radulović et al., 2022, Fildes et al., 2025). Reliance on accurate and high-quality data also limits the AHP method. Al Hazza et al. (2023) argues that although AHP effectively prioritizes influencing factors, the

reliability of its results depends heavily on the clarity and precision of input data. In this study, broadly available free-scale maps were used, while incorporating more detailed and accurate datasets could significantly improve the accuracy of the results.

7. CONCLUSION AND RECOMMENDATIONS

This study successfully applied the AHP for groundwater potential zone mapping in Sarpang District, Bhutan, by integrating seven thematic factors: geology, slope, land use/land cover, soil type, rainfall, lineament density, and drainage density. The AHP approach proved to be a cost-effective and efficient method for identifying and narrowing down areas with high groundwater potential. To support the interpretation of the AHP-based results, comparisons were made with ERT findings, which showed areas of general alignment, particularly in Pelrithang and Dzomlingthang. While not conclusive, this suggests that AHP can be a useful and cost-effective tool for preliminary groundwater assessment, offering strategic insights for planners and policymakers.

However, the results are not without limitations. A key concern lies in the subjectivity of weight assignment, which often depends on expert judgment. In this study, the consensus score among four experts was 55.8%, indicating low agreement and highlighting the potential for bias. Additionally, AHP assumes independence among influencing factors, which oversimplifies the complex, interrelated nature of hydrogeological variables. The reliance on freely available, coarse-resolution datasets further constrains the accuracy of the results. To mitigate these uncertainties, future studies should adopt consensus-based weighting methods, use high-resolution and site-specific data, and consider advanced hybrid approaches such as Fuzzy AHP or the Multi-Influencing Factor method to better capture factor interdependencies.

Ultimately, while AHP is a valuable tool for preliminary groundwater exploration, it should not replace detailed field investigations. Instead, it should be integrated with field-based validation methods such as ERT and bore well drilling to increase the accuracy and confidence of groundwater potential assessments. This integrated approach can significantly contribute to sustainable groundwater development and management in data-scarce regions like Sarpang, especially in the context of growing water demand and climate change.

REFERENCES

ACHU, A. L., THOMAS, J. & REGHUNATH, R. 2020. Multi-criteria decision analysis for delineation of groundwater potential zones in a tropical river basin using remote sensing, GIS and analytical hierarchy process (AHP). *Groundwater for sustainable development,* 10**,** 100365.

ADAMA, A., JUSCAR, N., MAMA, N., TSOPTIE, T., RACHIDA, B. & ELVIS, K. 2024. Delineation of groundwater potential zones using multi-criteria analysis (AHP), frequency ratios (RF), remote sensing and GIS: a case study of the Batcham municipality (west Cameroon). *Discover water,* 4**,** 75-20.

AHMED, A., RANASINGHE-ARACHCHILAGE, C., ALRAJHI, A. & HEWA, G. 2021. Comparison of Multicriteria Decision-Making Techniques for Groundwater Recharge Potential Zonation: Case Study of the Willochra Basin, South Australia. *Water (Basel),* 13**,** 525.

AL-DJAZOULI, M. O., ELMORABITI, K., RAHIMI, A., AMELLAH, O. & FADIL, O. A. M. 2021. Delineating of groundwater potential zones based on remote sensing, GIS and analytical hierarchical process: a case of Waddai, eastern Chad. *GeoJournal,* 86**,** 1881-1894.

AL HAZZA, M., AL DAHMANI, H., ALYAMMAHI, F., AL NAQBI, A., MALEQUE, A., ABDUL HALIM, N. F. H., SYED SHAHARUDDIN, S. I., MOHD ALI, A., AHMAD AZHAR, A. Z. & SARIFUDDIN, N. 2023. Study on the Challenges of Implementing Industry 4.0 in UAE Using Analytical Hierarchy Process AHP Method. Singapore: Springer.

ARULBALAJI, P., PADMALAL, D. & SREELASH, K. 2019. GIS and AHP Techniques Based Delineation of Groundwater Potential Zones: a case study from Southern Western Ghats, India. *Scientific reports,* 9**,** 2082-2082.

ATALLA, M. A., SHEBL, A., ĐURIN, B., KRANJČIĆ, N. & ALMETWALY, W. M. 2024. Assessment of groundwater potential zones in Kuwait's semi-arid region: a hybrid approach of multi-criteria decision making, Google earth engine, and geospatial techniques. *Scientific reports,* 14**,** 29938-23.

BEDEN, N., SOYDAN-OKSAL, N. G., ARıMAN, S. & AHMADZAI, H. 2023. Delineation of a Groundwater Potential Zone Map for the Kızılırmak Delta by Using Remote-Sensing-Based Geospatial and Analytical Hierarchy Processes. *Sustainability,* 15**,** 10964.

BHARGA, O. N. 1995. The Bhutan Himalaya: A Geological account. Special Publication 39.

DAS. 2018. *Sarpang Dzongkhag Profile* [Online]. Available: http://www.sarpang.gov.bt/about-dzongkhag [Accessed].

DERDOUR, A., BENKADDOUR, Y. & BENDAHOU, B. 2022. Application of remote sensing and GIS to assess groundwater potential in the transboundary watershed of the Chott-El-Gharbi (Algerian–Moroccan border). *Applied water science,* 12**,** 1-17.

DGM 2022. Groundwater Exploration using Electrical Resistivity Tomography.

DÍAZ-ALCAIDE, S. & MARTÍNEZ-SANTOS, P. 2019. Review: Advances in groundwater potential mapping. *Hydrogeology journal,* 27**,** 2307-2324.

DWLBC 2002. Assessing Agriculture Land: Agriculture land classification standards used in South Australia's land resource mapping program. *In:* DEPARTMENT OF WATER, L. A. B. C. (ed.). Government of South Australia.

FILDES, S. G., CLARK, I. F., BRUCE, D. & RAIMONDO, T. 2025. An ensemble model of knowledge- and data-driven geospatial methods for mapping groundwater potential in a data-scarce, semi-arid fractured rock region. *Applied water science,* 15**,** 86-33.

FILDES, S. G., CLARK, I. F., SOMARATNE, N. M. & ASHMAN, G. 2020. Mapping groundwater potential zones using remote sensing and geographical information systems in a fractured rock setting, Southern Flinders Ranges, South Australia. *Journal of Earth System Science,* 129**,** 160.

GIDAFIE, D., NEDAW, D. & AZAGEGN, T. 2024. Integrated remote sensing and geographic information system overlay analysis for groundwater potential evaluation using AHP and fuzzy AHP: Southern sections of the western Afar rift margin and associated rift floor. *Groundwater for sustainable development,* 26**,** 101310.

GMC. 2024. *Gelephu Mindfulness City* [Online]. Available: https://gmc.bt/about-us/ [Accessed 11/05/2025].

GOEPEL, K. D. 2018. Implementation of an Online Software Tool for the Analytic Hierarchy Process (AHP-OS). International Journal of the Analytic Hierarchy Process, Vol. 10 Issue 3 2018, pp 469-487,.

GUERRÓN-OREJUELA, E. J., RAINS, K. C., BRIGINO, T. M., KLEINDL, W. J., LANDRY, S. M., SPELLMAN, P., WALKER, C. M. & RAINS, M. C. 2023. Mapping Groundwater Recharge Potential in High Latitude Landscapes Using Public Data, Remote Sensing, and Analytic Hierarchy Process. *Remote sensing (Basel, Switzerland),* 15**,** 2630.

GULBET TEBEGE, E., MOLLA BIRARA, Z., GETAHUN TAKELE, S. & JOTHIMANI, M. 2025. Geospatial mapping and multi-criteria analysis of groundwater potential in Libo Kemkem watershed, upper blue Nile River basin, Ethiopia. *Scientific African,* 27**,** e02549.

GUPTA, D. S., BISWAS, A., GHOSH, P., RAWAT, U. & TRIPATHI, S. 2022. Delineation of groundwater potential zones, groundwater estimation and recharge potentials from

Mahoba district of Uttar Pradesh, India. *International journal of environmental science and technology (Tehran),* 19**,** 12145-12168.

GYELTSHEN, S., KANNAUJIYA, S., CHHETRI, I. K. & CHAUHAN, P. 2023. Delineating groundwater potential zones using an integrated geospatial and geophysical approach in Phuentsholing, Bhutan. *Acta geophysica,* 71**,** 341-357.

GYELTSHEN, S., TRAN, T. V., TEJA GUNDA, G. K., KANNAUJIYA, S., CHATTERJEE, R. S. & CHAMPATIRAY, P. K. 2020. Groundwater potential zones using a combination of geospatial technology and geophysical approach: case study in Dehradun, India. *Hydrological sciences journal,* 65**,** 169-182.

HOMTONG, N., PRINGPROH, W., SAKMONGKOLJIT, K., SRIKAROM, S., YAPUN, R. & WONGSAIJAI, B. 2024. Remote sensing-based groundwater potential evaluation in a fractured-bedrock mountainous area. *AIMS Geosciences,* 10**,** 242-262.

HÜMANN, M., SCHÜLER, G., MÜLLER, C., SCHNEIDER, R., JOHST, M. & CASPARI, T. 2011. Identification of runoff processes – The impact of different forest types and soil properties on runoff formation and floods. *Journal of hydrology (Amsterdam),* 409**,** 637-649.

ISHIZAKA, A. & LABIB, A. 2009. Analytic Hierarchy Process and Expert Choice: Benefits and limitations. *OR insight,* 22**,** 201-220.

JAAFARZADEH, M. S., TAHMASEBIPOUR, N., HAGHIZADEH, A., POURGHASEMI, H. R. & ROUHANI, H. 2021. Groundwater recharge potential zonation using an ensemble of machine learning and bivariate statistical models. *Scientific reports,* 11**,** 5587-5587.

KPIEBAYA, P., AMUAH, E. E. Y., SHAIBU, A.-G., BAATUUWIE, B. N., AVORNYO, V. K. & DEKONGMEN, B. W. 2022. Spatial assessment of groundwater potential using Quantum GIS and multi-criteria decision analysis (QGIS-AHP) in the Sawla-Tuna-Kalba district of Ghana. *Journal of hydrology. Regional studies,* 43**,** 101197.

LENTSWE, G. B. & MOLWALEFHE, L. 2020. Delineation of potential groundwater recharge zones using analytic hierarchy process-guided GIS in the semi-arid Motloutse watershed, eastern Botswana. *Journal of hydrology. Regional studies,* 28**,** 100674.

LONG, S., MCQUARRIE, N., TOBGAY, T., GRUJIC, D. & HOLLISTER, L. 2011. Geologic Map of Bhutan. *Journal of maps,* 7**,** 184-192.

MAIZI, D., BOUFEKANE, A. & BUSICO, G. 2023. Identification of groundwater potential zones using geospatial techniques and analytical hierarchy process (AHP): case of the middle and high Cheliff basin, Algeria. *Applied geomatics,* 15**,** 1005-1017.

MARTÍNEZ-SANTOS, P. & RENARD, P. 2020. Mapping Groundwater Potential Through an Ensemble of Big Data Methods. *Ground water,* 58**,** 583-597.

MUKHERJEE, P., SINGH, C. K. & MUKHERJEE, S. 2012. Delineation of Groundwater Potential Zones in Arid Region of India—A Remote Sensing and GIS Approach. *Water resources management,* 26**,** 2643-2672.

MURPHY, N. P., WATERHOUSE, H. & DAHLKE, H. E. 2021. Influence of agricultural managed aquifer recharge on nitrate transport: The role of soil texture and flooding frequency. *Vadose Zone Journal,* 20**,** n/a.

NCHM 2024. Climate Projection Report of Bhutan, Insights from CMIP6 Projections. *In:* NATIONAL CENTER FOR HYDROLOGY AND METEOROLOGY, R. G. O. B. (ed.). National Centre for Hydrology and Meteorology, Royal Government of Bhutan.

NEC 2016. National Integrated Water Resources Management Plan 2016.

NGWA. 2024. *National Ground Water Association: Facts About Global Groundwater Usage* [Online]. National Ground Water Association, United States Available: https://www.ngwa.org/what-is-groundwater/About-groundwater/facts-about-global-groundwater-usage [Accessed 10/05/2025 2025].

NOROOZ, R., NIVORLIS, A., OLSSON, P.-I., GÜNTHER, T., BERNSTONE, C. & DAHLIN, T. 2024. Monitoring of Älvkarleby test embankment dam using 3D electrical resistivity tomography for detection of internal defects. *Journal of civil structural health monitoring,* 14**,** 1275-1294.

NSB 2017. Population and Housing Census of Bhutan. *In:* NATIONAL STATISTICAL BUREAU, R. G. O. B. (ed.). NSB, Bhutan.

NSSC 2024. Technical Report on the Generation of National Soil Map of Bhutan Using Digital Soil MApping Techniques. *In:* DEPARTMENT OF AGRICULTURE, M. O. A. A. L. (ed.). NSSC, Department of Agriculture, Ministry of Agriculture and Livestock.

PANAHI, M. R., MOUSAVI, S. M. & RAHIMZADEGAN, M. 2017. Delineation of groundwater potential zones using remote sensing, GIS, and AHP technique in Tehran–Karaj plain, Iran. *Environmental earth sciences,* 76**,** 1-15.

PHOEMPHON, W. & TERAKULSATIT, B. 2023. Assessment of groundwater potential zones and mapping using GIS/RS techniques and analytic hierarchy process: A case study on saline soil area, Nakhon Ratchasima, Thailand. *AIMS geosciences,* 9**,** 49-67.

PIRASTEH, S., SAMAD, A., AHMAD, R., THAKURAL, L. N., KHAN, H. H., CHAUHAN, P., KHAN, A. & QAMAR, M. Z. 2025. Geospatial and AHP based identification of potential

zones for groundwater recharge in Haridwar District of India. *Frontiers in environmental science,* 13.

RADULOVIĆ, M., BRDAR, S., MESAROŠ, M., LUKIĆ, T., SAVIĆ, S., BASARIN, B., CRNOJEVIĆ, V. & PAVIĆ, D. 2022. Assessment of Groundwater Potential Zones Using GIS and Fuzzy AHP Techniques—A Case Study of the Titel Municipality (Northern Serbia). *ISPRS international journal of geo-information,* 11**,** 257.

RANI, M., PANDE, A., KUMAR, K., JOSHI, H., RAWAT, D. S. & KUMAR, D. 2022. Investigation of groundwater recharge prospect and hydrological response of groundwater augmentation measures in Upper Kosi watershed, Kumaun Himalaya, India. *Groundwater for sustainable development,* 16**,** 100720.

RUŽIČIĆ, S., KOVAČ, Z., PERKOVIĆ, D., BAČANI, L. & MAJHEN, L. 2019. The Relationship between the Physicochemical Properties and Permeability of the Fluvisols and Eutric Cambisols in the Zagreb Aquifer, Croatia. *Geosciences,* 9**,** 416.

SAATY, T. L. 1977. A scaling method for priorities in hierarchical structures. *Journal of mathematical psychology,* 15**,** 234-281.

SARANYA, T. & SARAVANAN, S. 2020. Groundwater potential zone mapping using analytical hierarchy process (AHP) and GIS for Kancheepuram District, Tamilnadu, India. *Modeling earth systems and environment,* 6**,** 1105-1122.

SARKAR, S. K., ESRAZ-UL-ZANNAT, M., DAS, P. C. & EKRAM, K. M. M. 2022. Delineating the groundwater potential zones in Bangladesh. *Water science & technology. Water supply,* 22**,** 4500-4516.

SHELAR, R. S., NANDGUDE, S. B., PANDE, C. B., COSTACHE, R., EL-HITI, G. A., TOLCHE, A. D., SON, C. T. & YADAV, K. K. 2023. Unlocking the hidden potential: groundwater zone mapping using AHP, remote sensing and GIS techniques. *Geomatics, natural hazards and risk,* 14.

SHIKLOMANOV, I. A. 1993. World freshwater resources. In: P.H. Gleick, ed. Water in crisis: a guide to the world's fresh water resources.

SINGH, L. K., JHA, M. K. & CHOWDARY, V. M. 2018. Assessing the accuracy of GIS-based Multi-Criteria Decision Analysis approaches for mapping groundwater potential. *Ecological indicators,* 91**,** 24-37.

TARIQ, M. A. U. R., WANGCHUK, K. & MUTTIL, N. 2021. A critical review of water resources and their management in Bhutan. *Hydrology,* 8**,** 31.

THAPA, M., YUDEN, K. & ACHARYA, S. 2022. Exploration of Groundwater Potential Zones: A Case Study In Phuentsholing. *Bhutan Journal of Research and Development.*

THONGLEY, T., CHOKI, T. & CHODEN, K. 2023. Groundwater Potential Mapping at Highly Populated Sub-districts of Thimphu District Using Fuzzy Analytic Hierarchy Process. *Applied Environmental Research,* 45.

TORGASHOV, E. V. (2012) *Imaging the subsurface in karst terrain using electrical resistivity tomography*. ProQuest Dissertations & Theses.

UN 2024. UN-Water Annual Report 2023.

USGS. 2014. *3D Elevation Program 30-Meter Resolution Digital Elevation Model (published 20142309, accessed March 03, 2025 at URL https://earthexplorer.usgs.gov/* [Online]. Available: https://earthexplorer.usgs.gov/ [Accessed].

WMD 2021. Assessment and Mapping of Water Sources/Springs in Bhutan: A comprehensive inventory and status of water sources used by Bhutanese communities.

YEH, H.-F., LIN, H.-I., LEE, S.-T., CHANG, M.-H., HSU, K.-C. & LEE, C.-H. 2014. GIS and SBF for estimating groundwater recharge of a mountainous basin in the Wu River watershed, Taiwan. *Journal of Earth System Science,* 123**,** 503-516.

APPENDICES

Appendix 1: Review of past Ground Water Potential studies to determine the frequency of influencing factors used for similar studies

SN	Literature	Rainfall	Lineament density	Drainage density	Geology	Slope	Soil	LULC	Elevation	Groundwater	Geomorphology	Temperature	Curvature	Recharge
1	(Atalla et al., 2024)	✓	✓	✓	✓	✓	✓	✓	x	✓	✓	✓	x	x
2	(Maizi et al., 2023)	✓	✓	✓	✓	✓	✓	✓	x	x	✓	x	x	x
3	(Adama et al., 2024)	✓	✓	✓	✓	✓	x	✓	✓	x	✓	x	x	x
4	(Gidafie et al., 2024)	x	✓	✓	✓	✓	✓	✓	x	x	x	x	x	✓
5	(Kpiebaya et al., 2022)	✓	✓	✓	✓	✓	✓	✓	x	x	x	x	x	x
6	(Gulbet Tebege et al., 2025)	✓	✓	✓	✓	✓	✓	✓	x	x	x	x	x	x
7	(Homtong et al., 2024)	x	✓	✓	✓	✓	✓	✓	✓	x	x	x	x	x
8	(Sarkar et al., 2022)	✓	✓	✓	✓	✓	✓	✓	x	x	✓	✓	✓	x
9	(Lentswe and Molwalefhe, 2020)	x	✓	✓	✓	✓	✓	✓	x	x	x	x	x	x
10	(Yeh et al., 2014)	x	✓	✓	✓	✓	x	✓	x	x	x	x	x	x
11	(Panahi et al., 2017)	✓	✓	✓	✓	✓	✓	✓	x	x	x	x	x	x
12	(Mukherjee et al., 2012)	✓	✓	✓	✓	✓	✓	✓	x	x	✓	x	x	x
13	(Gupta et al., 2022)	✓	✓	✓	✓	✓	✓	✓	x	x	✓	x	x	x
14	(Derdour et al., 2022)	✓	✓	✓	✓	✓	✓	✓	✓	x	x	x	x	x
15	(Al-Djazouli et al., 2021)	✓	✓	✓	✓	✓	x	✓	✓	✓	✓	✓	✓	✓
16	(Achu et al., 2020)	x	✓	✓	✓	✓	✓	✓	x	x	✓	x	x	x
17	(Arulbalaji et al., 2019)	✓	✓	✓	✓	✓	✓	✓	x	x	✓	x	x	x
18	(Singh et al., 2018)	x	x	✓	✓	✓	x	x	x	x	x	x	x	x
19	(Jaafarzadeh et al., 2021)	✓	x	✓	✓	✓	✓	✓	x	x	x	x	✓	x
20	(Guerrón-Orejuela et al., 2023)	✓	x	✓	✓	✓	✓	✓	x	x	x	x	x	x
21	(Martínez-Santos and Renard, 2020)	x	x	✓	✓	✓	✓	✓	✓	x	x	x	x	x
	Total	14	17	21	21	21	17	20	4	1	7	2	3	1